Chemistry Europe
European Chemical Societies Publishing

WILEY VCH

Excellence in Chemistry Research

Announcing our new flagship journal

- Gold Open Access
- Publishing charges waived
- Preprints welcome
- Edited by active scientists

Meet the Editors of *ChemistryEurope*

Luisa De Cola
Università degli Studi di Milano Statale, Italy

Ive Hermans
University of Wisconsin-Madison, USA

Ken Tanaka
Tokyo Institute of Technology, Japan

ChemPlusChem

Research Article
doi.org/10.1002/cplu.202300183

Chemistry Europe
European Chemical Societies Publishing

www.chempluschem.org

Carbon Dioxide Cycloaddition to Epoxides Promoted by Nicotinamidium Halide Catalysts: A DFT Investigation

Valeria Butera*[a, b]

The utilization of CO_2 as building block for the production of cyclic carbonate is a promising route to simultaneously mitigate the global warming issue and obtain valuable commercial chemicals. In this work, the activity of nicotinamidium halide catalysts towards the CO_2 conversion into cyclic carbonate has been explored by means of density functional theory (DFT) calculations. DFT calculations support the ability, suggested experimentally, of the pyridium α-C–H proton of the catalysts to activate the epoxide ring *via* a hydrogen bond. Interestingly, DFT calculations underline the involvement of the *n*-octyl substituent of the pyridyl ring in the epoxide activation, while the hydrogen atom of the amide group N–H is rather involved in the stabilization of the iodide trough electrostatic interactions. Moreover, the replacement of the pyridium α-C–H proton with the bulkier methyl group leads to a different reaction mechanism. The calculated energy barriers well reproduce the experimental trends of the studied catalysts, and the computed activation barrier of 29.0 kcal/mol, relative to the ring opening step of the most active catalyst, is in line with the experimental working temperature of 80 °C. Those results shed light on the CO_2 fixation reaction contributing to the development of more efficient catalytic systems.

Introduction

CO_2 removal from the atmosphere can help mitigate the global warming issue and act as a non-toxic, abundant and cheap carbon building block for the production of added-value chemicals and fuels.[1–4] The main challenge relies on the development of efficient routes that make the CO_2 conversion a commercial process.[5] In this regard, the high thermodynamic stability of the CO_2 molecule hinders its conversion, which is only possible under the utilization of a catalyst. Efficient routes for the production of methanol,[6–12] methane,[13–15] carbon monoxide,[16,17] and dimethyl ether[18] have been reported, and the involved conversion reaction have been studied by both experimental and theoretical methods.

Among the desired CO_2 conversion products, cyclic carbonates have received great attention due to their high commercial value.[19–24] The chemical reaction, known as CO_2 fixation into epoxides, involves three main steps: 1) epoxide ring activation and opening; 2) CO_2 insertion and 3) ring closure and release of the product.[25–27] However, for each of these steps to take place, a catalyst needs to be added to the reaction system. Therefore, efficient catalysts should possess good nucleophilic character in order to be able to activate the epoxide ring and facilitate its opening, and good capability as leaving group to speed up the ring closure step. Several catalytic systems have shown high activity and stability for this reaction, including ionic liquids,[28–30] bifunctional or binary complexes,[31–33] and quaternary onium salts.[26,34]

Kleij et al.[35,36] have discovered that the establishment of a hydrogen bond between a phenolic compound and the epoxide activates the oxirane ring towards the nucleophilic attack of the nBu_4NI cocatalyst, thus quantitatively forming the cyclic carbonate product under mild reaction condition. Based on their findings, several hydrogen bond donor (HBD) catalysts, including both O–H and N–H groups, have been proposed.[37–39] Recently, compounds containing relatively weak C–H HBD[40] and halogen bond donors[41,42] were also found to efficiently convert epoxides into the corresponding cyclic carbonates. Moreover, the presence of weak HBDs rather than strong ones has been suggested as more appropriate in the carbon cycloaddition into epoxide (CCE) catalysis. In this regard, Gao *et al.*[43] have explored the use of primary and secondary carboxamides as promising HBD catalysts. The catalytic system proposed by the authors consists of an ideal molecular nicotinamide (1) scaffold where the two main moieties of the HBD and onium halide, necessary for CCE reactions, are essentially installed in one-component HBD/onium halide catalyst. Starting from the nicotinamide, both the N of pyridine ring and the amide NH_2 of 3-carbamoyl group were modified by formal alkylation to produce a new family of nicotinamidium halide catalysts, labeled by the authors as **2**, in which both the R1, R2 and R3 are substituted with different alkyl groups. Among all the explored **2**-derived catalysts, 1-*n*-octyl nicotinamidium halides **2d** (see Figure 1) was reported as the optimal catalyst with the highest styrene carbonate yield of 96% at 80 °C. The authors

[a] *Dr. V. Butera*
CEITEC – Central European Institute of Technology Central European Institute of Technology
Purkyňova 123
Brno 612 00 (Czech Republic)
E-mail: butera@vutbr.cz
[b] *Dr. V. Butera*
Department of Science and Biological Chemical and Pharmaceutical Technologies
University of Palermo
90128 Palermo (Italy)

Supporting information for this article is available on the WWW under https://doi.org/10.1002/cplu.202300183

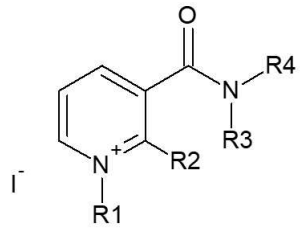

2d: R1= *n*-octyl; R2 = R3 = R4 = H
2i: R1= *n*-octyl; R2 = CH_3; R3 = R4 = H
2j: R1= *n*-octyl; R2 = H; R3 = R4 = CH_2CH_3

Figure 1. Structures of the **2d**, **2i** and **2j** investigated nicotinamidium iodide catalysts.

suggest that catalyst **2d** can activate the epoxide ring *via* a bidentate hydrogen bonding involving the Hα of the non-classical α-C–H of the quaternary pyridinium and the Hβ of the amide N–H group, while the halide acts as the nucleophile in the ring opening step. The importance of both Hα and Hβ in activating the epoxide via a bidentate coordination has been validated by designing the nicotinamidium iodide catalysts **2i** with blocked α-C–H (Hα replaced by a methyl group), and **2j** with blocked N–H (Hβ replaced by ethyl groups), as depicted in Figure 1.

Experimentally, it is found that the catalytic activity of **2i** and **2j** is reduced to 61 and 47 %, respectively. The activity of **2i** is exactly the same as that obtained using nicotinamide and tetrabutylammonium (**TBAI**), while that of **2j** is similar to **TBAI** alone. On the basis of the notably reduced activity of Hα and Hβ blocked systems, the importance of the bidentate H-bond donor mode for an optimal catalytic performance is suggested by the authors. Moreover, the similar activity of **2j** to TBAI, suggest that the α-C–H in **2j** is inactive probably due to steric hinderance of the adjacent N–Et_2, while the slightly higher activity of **2i** with respect to **2j**, denotes that N–H is an active HBD site.

In this study, density functional theory (DFT) calculations have been employed to investigate the different nature of the pivotal hydrogen bonding established between the **2i** and **2j** blocked systems with the styrene epoxide (SO), and compared it with that found in the more active **2d** catalyst. In order to get a comprehensive understanding of the HBD/activity relationship, the investigation was extended to nicotinamide and **TBAI** system. Eventually the whole CO_2 fixation reaction of epoxide to cyclic carbonate was investigated. The herein presented results support the formation of a bidentate H-bond donor mode in activating the epoxide ring. However, DFT calculations underline the involvement of the non-classical α-C–H of the quaternary pyridinium along with one H atom of the n-butyl group for the ring activation, while the amide N–H group interacts and stabilizes the Iodide anion. As a consequence, the inclusion of a bulkier NEt_2 group in **2j** does not have any influence in the epoxide activation mode and conversion mechanism as compared to **2d**, but its presence contributes to lower the nucleophilic character of the former catalyst, increasing the activation barrier involved in the ring opening step. Interestingly, due to the pivotal role of Hα, its replacement with the bulkier CH_3 group leads to a different reaction mechanism.

Results

Optimized structures of the different catalytic systems and their interaction with SO.

Figure 2 shows the optimized structures of all the investigated systems. As it can be seen from Figure 2a, in the nicotinamide-TBAI adduct (**1-TBAI**), the iodide established two hydrogen bonds with the Hα of the non-classical α-C–H of the quaternary pyridinium and the Hβ of the amide group, whose calculated distances are 3.08 and 2.77 Å, respectively. The

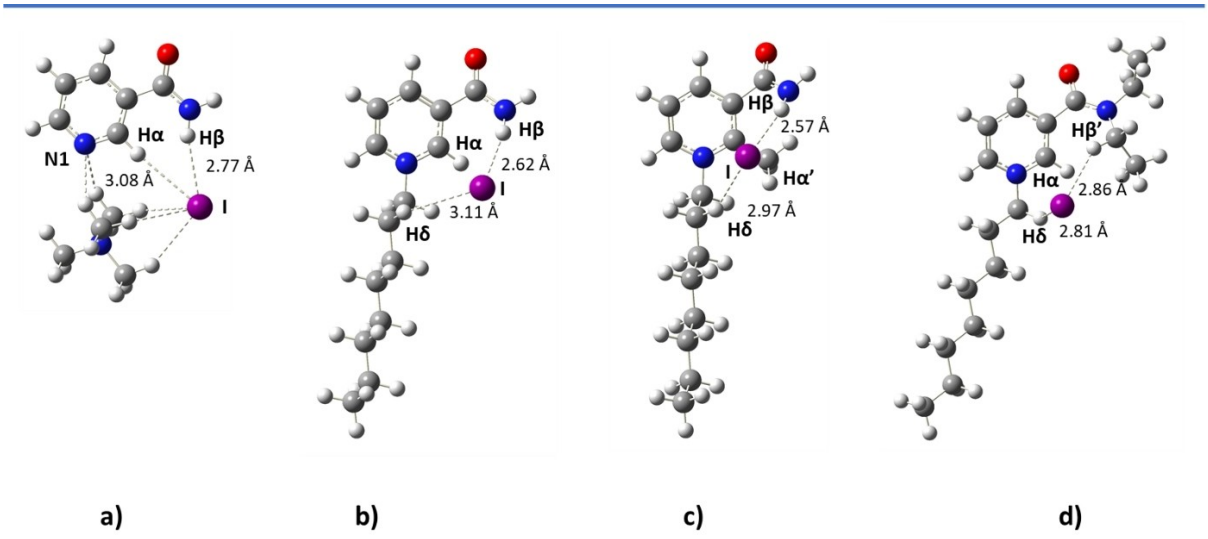

Figure 2. Optimized structures of a) **1-TABI**; b) **2d**; c) **2i** and d) **2j** catalysts.

butylammonium cation interacts with the N1 of the pyridine ring through two hydrogen bonds involving two hydrogen atoms of the methyl groups, while the other two hydrogen atoms of the same groups further interact with the iodide. The planar geometry of the nicotinamide molecule is distorted in all the other three investigated derivatives (**2d**, **2i** and **2j**). Indeed, the optimized structure of **2d**, shown in Figure 2b, underlines that the amide group of the nicotinamide is rotated by 25° with respect to the pyridine ring. As a consequence, the interaction between Hα and the iodide is lost and replaced by a hydrogen bond with the Hδ hydrogen atom of the n-octyl substituent with a computed distance of 3.11 Å, while the second hydrogen bond involving Hβ is kept and becomes stronger, as underlined by the computed shorter distance of 2.62 Å. Gao *et al.*[43] report the ^{1}H NMR spectrum of the pure catalyst **2d**, which shows an abnormal chemical shift of the Hα proton at 10.65 ppm. The authors suggest a negligible hydrogen bond interaction between the iodide atom and the proton, with a consequent deshielding effect of the latter, while the iodide should be located on top of the pyridinium ring, establishing a π interaction with the pyridine ring. In agreement with the experimental findings, our calculations support the lack of interaction between the iodide anion and Hα. However, our calculations show that the suggested π interaction does not take place and the negative charge of the anion is instead stabilized by the two hydrogen bonds described above. In order to further support the reliability of those results, the structure of **2d** catalyst has been optimized at the ω-B97XD level of theory, which include dispersion forces. The Hδ and I–Hβ elongate from 3.11 to 3.23 Å, and from 2.62 to 2.73 Å, thus supporting the nature of weak interactions between iodide and nicotinamide found with PBE0. It is worth to mention that weak interactions between hydrogen atoms of nicotinamide derivatives and iodide are highly beneficial, since they allow for a more "free" nucleophile, thus favoring the ring opening step.

Due to the lack of interactions between I^- and Hα, replacing the latter with a methyl group as in **2i** has no significant influence on the nature of the cation/anion adduct. However, the higher steric hindrance of CH_3 with respect to H, implies the increase of the rotation of the amide group with a computed dihedral angle of 52.8° (see Figure 2c), while shorter bond distances of 2.97 and 2.57 Å are calculated for Hδ–I and Hα′–I, respectively.

Similarly to the previous cases, when NH_2 is replaced by N(Et)2, as in **2j**, the iodide anion establishes two interactions with the Hδ hydrogen atom of the *n*-octyl group, and a second one with Hβ′ of the ethyl substituent of the amide. Due to the bulkier ethyl groups, the I–Hβ′ interaction becomes longer, and the iodide is moved towards the *n*-octyl substituent, shortening the I–Hδ distance. The calculated distances are 2.81 and 2.86 Å, respectively, which are the shortest and longest distances among the three catalysts.

The potential of all the catalysts discussed above to act as hydrogen bond donor and activate the O ring has been investigated. When a molecule of SO is added to the **1-TBAI** catalyst two structures are found, named Int1(**1-TBAI**)′ and Int1(**1-TBAI**), which are shown in Figure 3. In the first one, the O1 oxygen of the epoxide interacts with Hγ hydrogen of the nicotinamide with a calculated O1–Hγ distance of 1.97 Å (see Figure 3a), while the negative charge of the iodide is stabilized trough the interaction with Hα and Hβ. In the second case, the iodide anion is replaced by the epoxide, with the consequent formation of two hydrogen bonds Hα–O1 and Hβ–O1 whose calculated distances are 2.43 and 1.90 Å, respectively. The negative charge of the iodide is instead stabilized via electrostatic interaction with the nearby tetrabutylammonium cation and Hγ. This latter intermediate is slightly more stable than the previous one, indicating that the bidentate coordination of the epoxide is favorable, and therefore in presence of **TBAI**, nicotinamide acts as a bidentate HBD activating the epoxide ring through two hydrogen bonds.

The optimized structures of all the three intermediates Int1(**2d**), Int1(**2i**) and Int1(**2j**) (see Figure 4) show that the epoxide is activated by the formation of two hydrogen bonds with the 1-n-octyl nicotinamidium. Particularly, in Int1(**2d**), the O1 oxygen atom of the epoxide interacts with the Hδ and Hα with calculated distances of 2.33 and 2.18 Å, respectively. When the H atoms of the amide are replaced by the bulkier Et groups, the Hδ–O1 distance is elongated of 0.25 Å, while the computed Hα–O1 remains unchanged. On the other hand, the replacement of the Hα with the methyl group leads to an elongation

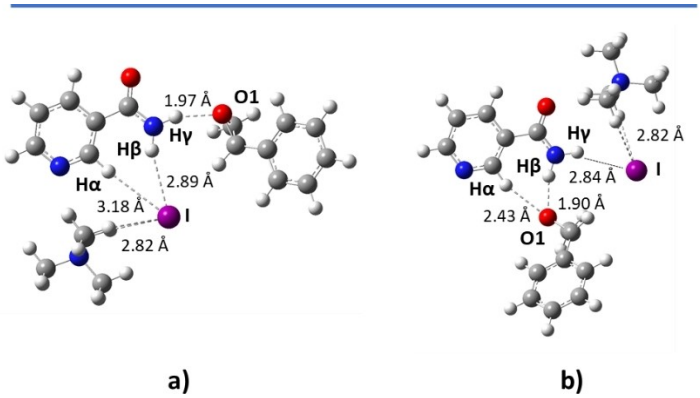

Figure 3. Optimized structures of a) Int1(**1-TBAI**)′ and b) Int1(**1-TBAI**).

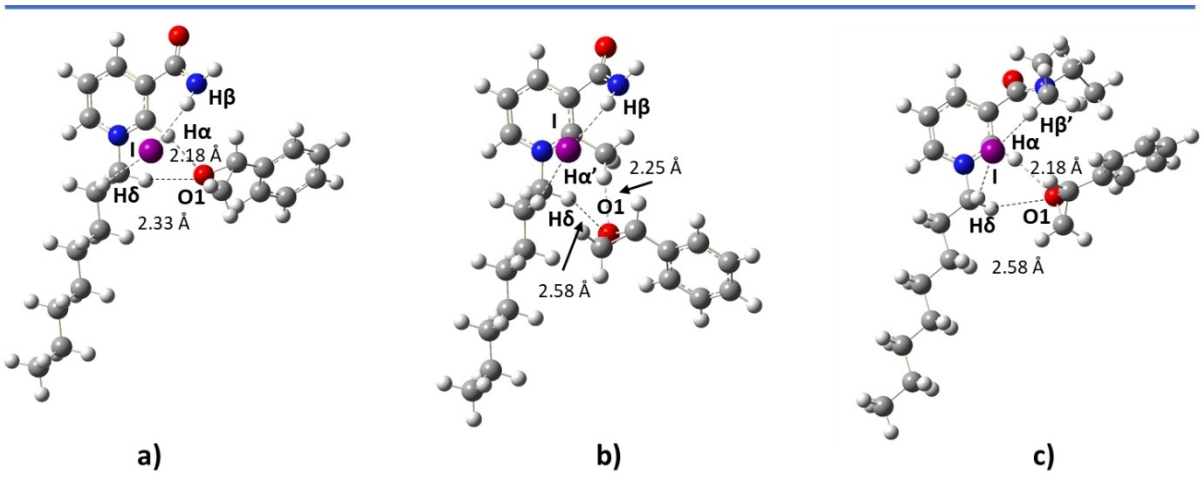

Figure 4. Optimized structures of a) Int1(**2 d**), b) Int1(**2 i**) and c) Int1(**2 j**).

of 0.25 and 0.07 Å of the corresponding Hδ–O1 and Hα′–O1 distances with respect to Int1(**2 d**).

PO conversion into PC

2d. Experimental studies have shown that **2 d** catalyst is the most efficient among all the studied catalysts. The optimized structures of all the intercepted stationary points involved in the CO_2 fixation reaction are shown in Figure S2 of the supporting information, while the schematic representation along with the potential energy surface (PES) are shown in Figure 5. After the activation of the epoxide by coordination to the HBD, as described above, the reaction proceeds by the nucleophilic attack of the iodide at the methylene carbon leading to the ring-opening and consequent formation of the alkoxide anion (Int2(**2 d**) in Figure 5). The calculated energy barrier with respect to Int1(**2 d**) is 29.0 kcal/mol and involves

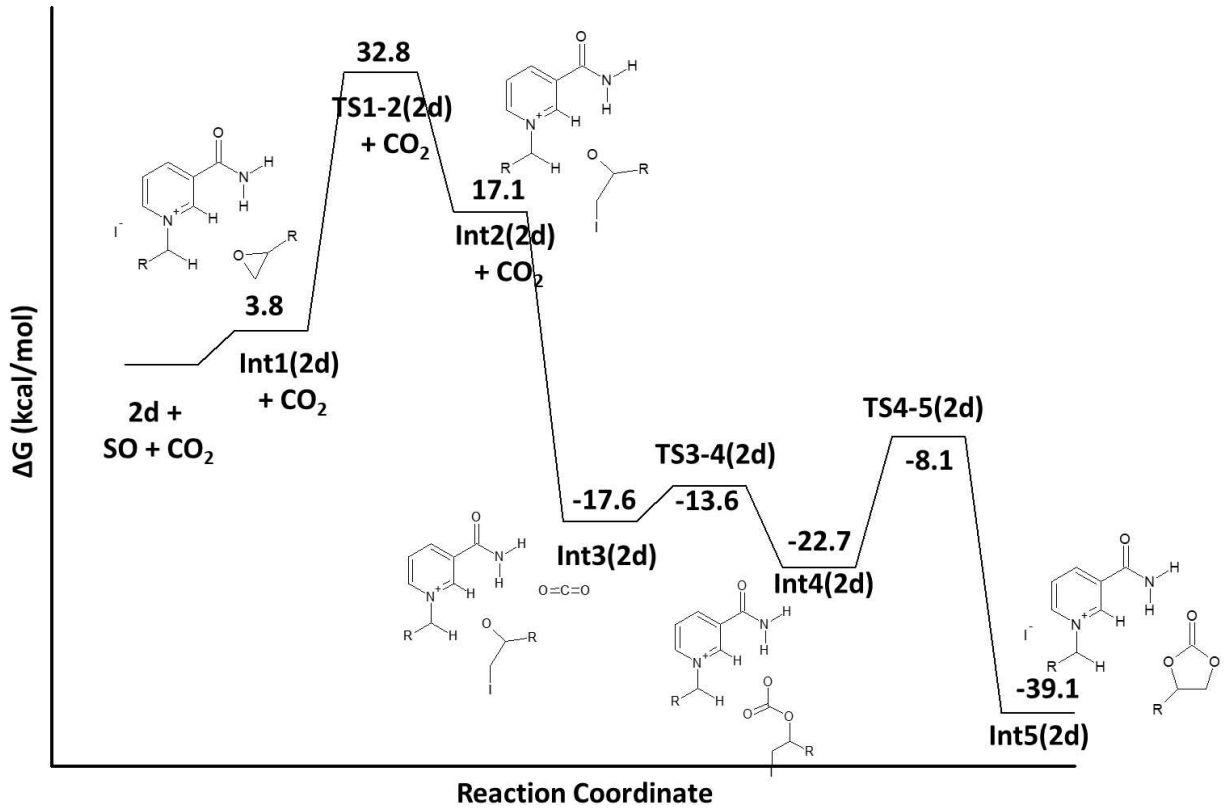

Figure 5. Potential energy surface of the CO_2 fixation into SO to form SC in presence of **2 d**.

TS1-2(**2d**), whose calculated imaginary frequency is 425.32 *i*cm^{-1} and it is clearly associated to the simultaneous breaking of the C–O bond and formation of I–C bonds. The alternative nucleophilic attack of the iodide at the most substituted carbon of SO has also been explored. However, all the attempts to intercepts the corresponding transition state have failed, suggesting that this route should be rule out. In the formed Int2(**2d**) the planar geometry of the nicotinamidium is restored and the intermediate is found to be endergonic of 17.1 and 13.3 kcal/mol with respect to the separated reactants and Int1(**2d**), respectively. The alkoxide anion establishes two electrostatic interactions with the Hα and Hβ atoms of the nicotinamide, whose calculated distances are 1.59 and 1.66 Å, respectively. However, the C–Hα distance is drastically elongated from 1.08 Å in both **2d** and Int1(**2d**) to 1.14 Å in Int2(**2d**). On the other hand, when the molecule of CO_2 is added to the reaction system, the formed Int3(**2d**) becomes exergonic of 17.6 kcal/mol with respect to the separated reactants, and 34.7 kcal/mol more stable than the previous intermediate Int2(**2d**). The activation of the CO_2 molecule is underlined by the slight deviation of the O–C–O angle in Int2(**2d**) from its linearity to the value of 172°, along with an elongation of one of the two C=O bond distances from 1.16 to 1.17 Å. Thanks to that, the CO_2 insertion into the alkoxide becomes a very easy step, involving an activation energy of only 4.0 kcal/mol with respect to Int3(**2d**). In the optimized structure of the involved transition sate, TS3-4(**2d**), the computed distance between the epoxide oxygen O1 and the carbon of the CO_2 is 2.05 Å, while the calculated O–C–O angle of the carbon dioxide is 156°. The formed carbonate anion Int4(**2d**) is 5.1 kcal/mol more stable than Int3(**2d**), lying at 22.7 kcal/mol below the reactants' asymptote. In this intermediate, the delocalized negative charge of the carbonate anion is stabilized by hydrogen bonding with Hα, Hβ and Hδ, whose calculated distances are 1.78, 1.73 and 2.17 Å, respectively. In the last step of the reaction, the cyclic carbonate product is obtained by the release of the iodide and the consequent formation of a new C–C bond. The so-formed Int5(**2d**) intermediate is highly exergonic and lies at 39.1 and 16.4 kcal/mol below the separated reactants and Int4(**2d**), respectively. The optimized structure of Int5(**2d**) underlines the presence of two hydrogen bonds between the carboxylic oxygen of SC with Hα and Hδ, whose calculated values are 2.16 and 2.21 Å, while Hβ re-establishes an interaction with the released iodide anion (2.62 Å). The step occurs via TS3-4(**2d**), with a calculated imaginary frequency is 428.11 *i*cm^{-1} and an energy barrier of 14.6 kcal/mol with respect to Int4(**2d**). It is worthy to mention that the overall reaction relies on the mobility of both the iodide and epoxide, which have to match suitable positions to favor the iodide nucleophilic attack in the first step, and the recovery of the of the initial catalyst in the last one. However, the fast movement of those species is highly reasonable, especially at the experimental temperature of 80 °C.

Due to the very low barrier involved in the CO_2 insertion step, a different mechanism in which the ring opening and CO_2 insertion occur simultaneously has also investigated. In this case, the first intermediate is Int1′(**2d**), whose structure is shown in Figure S2, obtained by the addition of the CO_2 molecule to Int1(**2d**). As for the Int3(**2d**) discussed above, also in this case, the addition of the CO_2 to the reaction system contribute to significantly lower the energy of the formed intermediate, which lies at 29.2 kcal/mol below the reaction asymptote. The optimized structure of the corresponding transition state, TS1′-3(**2d**) underlines that the CO_2 molecule is kept at the same distance as in Int1′(**2d**) and the computed O–C–O angle is also identical (178°). In other words, the CO_2 molecule is not activated in this step, and the concerted ring opening and CO_2 insertion mechanism should be discarded. This conclusion is also emphasized by the computed activation barrier of 30.8 kcal/mol between Int1′(**2d**) and TS1′-3(**2d**), which is almost equivalent to that obtained for the system in absence of CO_2. Moreover, the analysis of the intrinsic reaction coordinate (IRC) of TS1′-3(**2d**) shows that the CO_2 is not directly coordinated thus confirming the two step mechanisms.

The energetic span model (ESM), whose details are described in the Experimental section, has been applied. By looking at the PES of the two-step mechanism, we can identify the rate determining intermediate (TDI) as Int1(**2d**) and the rate determining transition state (TDTS) as TS1-2(**2d**) with a computed öE of 29.0 kcal/mol.

Rostami and co-workers[22] have recently explored the utilization of non-toxic and inexpensive pyridine carboxylic acids as efficient catalytic systems for the CO_2 insertion into epoxide. The authors calculate energy barriers of 18.6 and 9.8 kcal/mol for the ring opening and ring closing steps, respectively, which are both lower than those presented in this work. However, it is worthy to note that, in Rostami's work, experiments were performed at a lower working temperature of 50 °C. Moreover, both the studies underline that the opening of the epoxide ring is the most unfavored step. Arayachukiat *et al.*[21] calculated energy barriers of 13.0 (ring opening) and 15.6 (ring closure) kcal/mol for the PO conversion into PC in presence of ascorbic acid. Experimentally, the authors achieved PO conversions of 70 and 94% at room and 40 °C temperatures, respectively. Those results underline the correspondence between the calculated energy barriers and the experimental working temperature, showing that higher energy barriers are associated to higher experimental temperature.

When **2d** is replaced by **2j**, the fixation reaction occurs following a very similar mechanism. The calculated energy barrier for the iodide nucleophilic attack at the carbon of the epoxide is 39.4 kcal/mol with respect to the intermediate Int1(**2j**) (see Figure 6), which is 10.4 kcal/mol higher than that calculated for the **2d** catalyst. In the formed Int2(**2j**) intermediate (shown in Figure S5 along with the optimized structures of all the stationary points), two hydrogen bonds are formed between the O1 oxygen of the alkoxide anion and the α-C–H, Hα, and Hδ of the *n*-butyl chain, whose calculated distances are 1.93 and 1.64 Å, respectively. Similarly to the **2d** case, the nicotinamidium structure of Int2(**2j**) is planar and the intermediate is found to be endergonic with respect to the reactants' asymptote of 21.2 kcal/mol. The inclusion of the CO_2 molecule leads to the formation of Int3(**2j**), in which the carbon dioxide is slightly distorted from its linear structure with a computed O–C–O angle of 170.7 and the distance between the

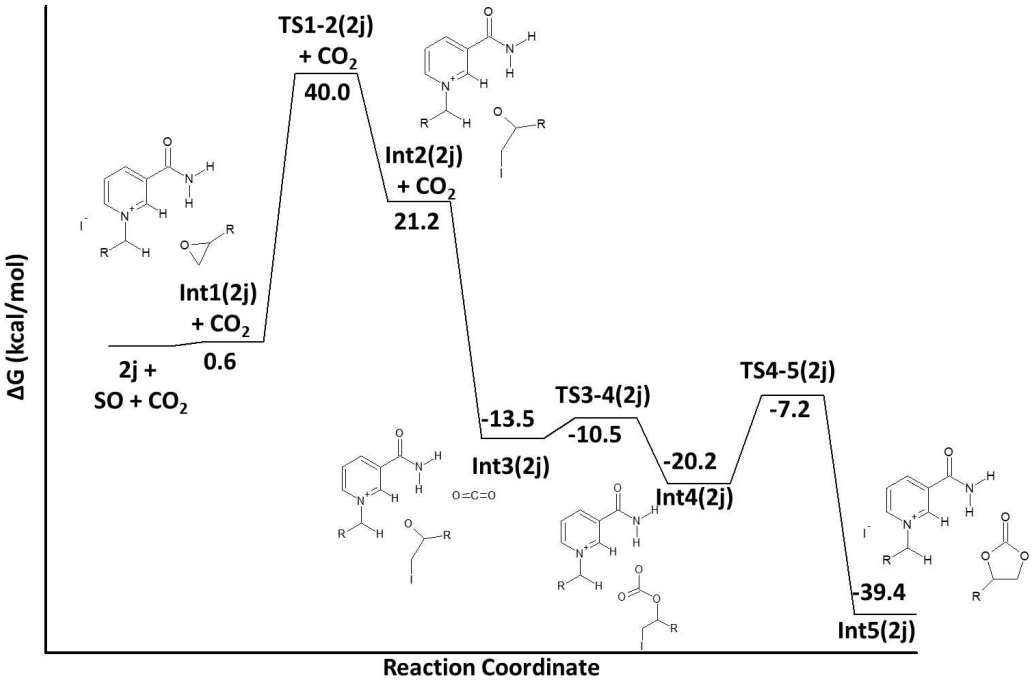

Figure 6. Potential energy surface of the CO_2 fixation into SO to form SC in presence of **2j**.

epoxide oxygen and the carbon atom is 2.47 Å. In accordance with the **2d** case, Int3(**2j**) is exergonic with respect to the reactants' asymptote of 13.5 kcal/mol, while the activation barrier for the CO_2 insertion step is even lower than that calculated for **2d** catalyst and corresponds to 2.9 kcal/mol. The optimized structure of the formed Int4(**2j**), which lies at 20.2 kcal/mol below the separated reactants (and 13.5 kcal/mol below the previous intermediate Int3(**2j**)), shows that the carboxylic oxygen interacts with Hα and Hβ' of the NEt groups. The calculated distances are 1.77 and 2.25 Å, respectively. The ring closure step involves an energy barrier of 12.3 kcal/mol and the formed intermediate which includes the cyclic carbonate product is exergonic of 39.4 kcal/mol. In accordance with the previous **2d** case, a concerted mechanism does not occur and the CO_2 molecule acts as a spectator during the ring opening step as confirmed by the IRC calculation.

The application of the ESM to the calculated PES allows for the identification of the TDI and TDTS as Int1(**2j**) and TS1-2(**2j**), respectively, with a computed öE of 39.4 kcal/mol.

We have calculated the empirical nucleophilicity index, N, following the model suggested by Jaramillo *et al.*[44] (details are given in the Supporting Information). DFT results show that the calculated nucleophilic index of Int1(**2d**) is 0.4 eV higher than that of Int1(**2j**), thus suggesting a marked nucleophilic character of the former and explaining the lower calculated activation barrier.

2i. The CO_2 fixation into PO in presence of **2i** catalyst has been also investigated. DFT results suggest that the replacement of the α-C–H proton of the pyridine ring with the bulkier methyl group has influence on the involved reaction mechanism. Particularly, the optimized structure of the first transition state, TS1-2(**2i**) underlines that the nucleophilic attack of the iodide at the carbon of the epoxide ring occurs simultaneously to the Hα' transfer of the methyl group to the O1 oxygen of the SO. An imaginary frequency of 378.46 *i*cm^{-1} has been calculated with a corresponding energy barrier of 39.3 kcal/mol (see Figure 7). The so-formed Int2(**2i**), which lies at 11.9 kcal/mol above the reactants' asymptote, is 5.2 and 9.3 kcal/mol more stable than the analogous Int2(**2d**) and Int2(**2j**), respectively. The optimized structure, reported in Figure S3, shows that the Hα' is transferred to the O1 of the alkoxide anion, while the planar geometry of the nicotinamidium is not restored due to the hindrance of the CH_2^- group. The addition of the CO_2 molecule to the reaction system leads to the formation of Int3(**2i**), whose calculated energy is 19.6 and 31.5 kcal/mol lower than the separated reactants and Int2(**2i**), respectively. The protonation of the epoxide oxygen decreases its nucleophilic character and, consequently, hinders the CO_2 insertion step. The corresponding activation energy is 16.9 kcal/mol, which is indeed 12.9 and 14.0 kcal/mol higher than those obtained for **2d** and **2j**, respectively. In the formed Int4(**2i**), the negative charge of the oxygen of the newly carboxylic group is stabilized by the interactions with the Hα' atom of the methyl and Hδ of the *n*-butyl group, whose calculated distances are 1.93 and 2.08 Å, respectively. The last step involves the ring closure which occurs via TS4-5(**2i**), with a calculated activation barrier of 13.9 kcal/mol. The formed intermediate, containing the SC product, lies at 38.8 kcal/mol below the separated reactants.

The possibility that the reaction occurs *via* a concerted mechanism in which the ring opening and CO_2 insertion occur simultaneously has also been explored. In analogy with the previous cases, the reference intermediate for this mechanism is Int1(**2i**)', that is obtained by adding one molecule of carbon

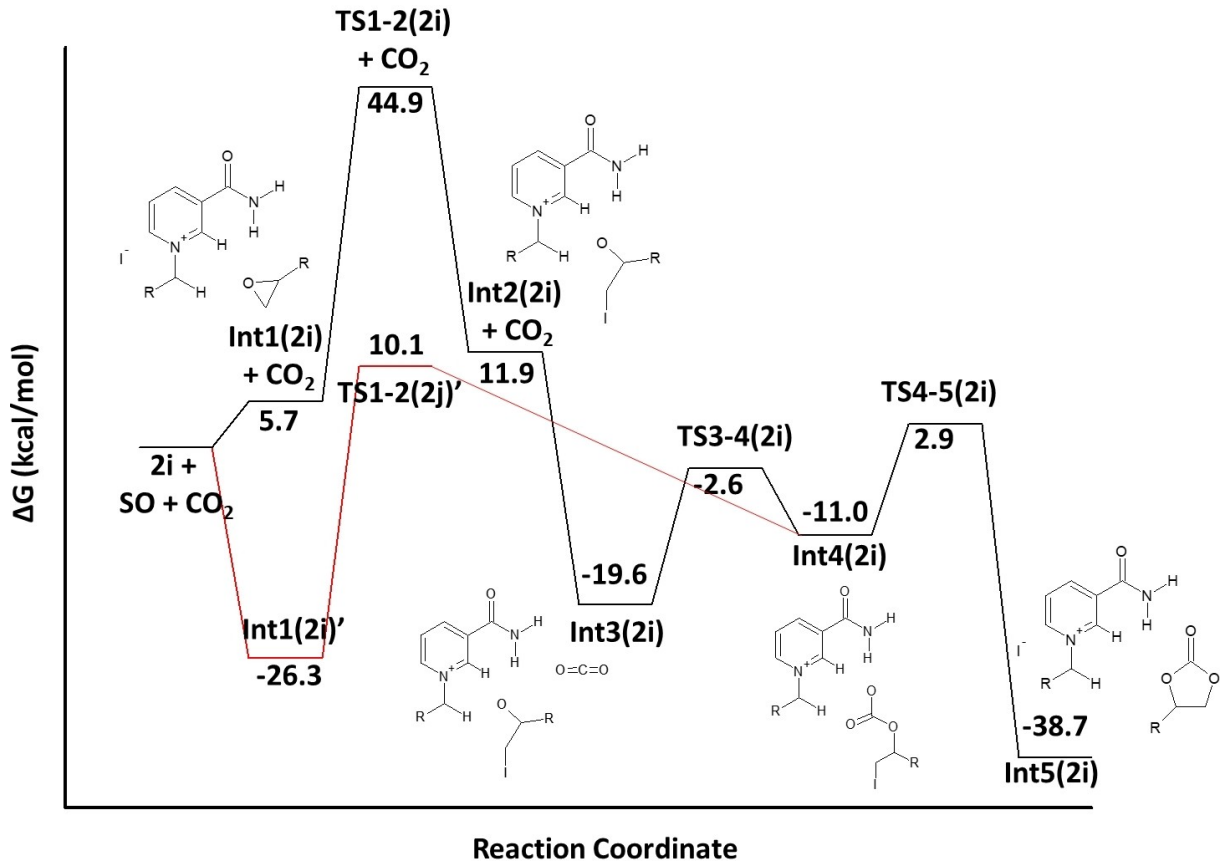

Figure 7. Potential energy surface of the CO_2 fixation into SO to form SC in presence of **2i**.

dioxide to Int1(**2i**). The optimized structure of TS2′-4(**2i**) underlines that the calculated O–C–O angle deviates from its linearity, becoming 164.2°, while the O–C distance between the O1 of the SO and the carbon of the CO_2 is 2.57 Å. Moreover, the IRC calculation clearly shows that the CO_2 molecule is moved closer to the open epoxide while its O–C–O is decreased, thus underlying the direct activation of the carbon dioxide. Starting from the last geometry of the IRC calculation, we fully relaxed the structure obtaining Int4(**2i**). These results suggest that in presence of catalyst **2i** the concerted mechanism is possible and favored with respect to the two steps mechanism.

By applying the ESM at the concerted mechanism, a δE of 36.4 kcal/mol is calculated between the Int1(**2i**)′ (TDI) and TS1-2(**2i**)′ (TDTS). The computed nucleophilic index of Int1(**2i**)′ is 4.3 eV, which is 0.3 and 0.1 lower and higher with respect to Int1(**2d**) and Int1(**2j**), respectively.

Conclusions

A DFT investigation was carried out to investigate the role of hydrogen bonding in activating and converting styrene epoxide into the corresponding styrene carbonate in presence of nicotinamide halide organo-catalysts. In agreement with the experimental findings, DFT calculations support the crucial role of the α-C–H (Hα) in the activation of the epoxide. However, DFT results show that the Hβ and Hβ′ of the NH_2 and NEt_2 groups of the amide do not participate to the epoxide activation, but they are rather involved in the stabilization of the iodide trough electrostatic interactions. On the other hand, a crucial role is played by the Hδ of the *n*-octyl substituent which is indeed involved in the formation of an additional hydrogen bond with the epoxide, thus contributing to its activation. Therefore, similar reaction mechanisms are found for **2d** and **2j** catalysts, with the former involving a lower δE that supports the better catalytic activity reported experimentally, as also supported by the higher calculated nucleophilic index. On the other hand, due to the involvement of Hα in each step of the fixation reaction, its replacement with the bulkier CH_3 group implies a different reaction mechanism.

Experimental

All the calculations have been performed using GAUSSIAN 16 code[45] and selecting the hybrid PBE0 functional.[46–49] However, preliminary tests were carried out on **2d** catalyst using ω-B97XD, in order to evaluate the influence of including dispersion forces in predicting the strength of the I···H interactions, which are crucial for these systems. For the optimization of all the structures, the standard 6-31G* basis sets of Pople and co-workers were employed for the all the atoms, except I for which the relativistic compact Stuttgart/Dresden (SDD) effective core potential[50] was used.

However, single point calculations based on the relaxed geometries were performed employing the more extended 6-311 + G** basis sets in order to get more accurate free energies. Frequency analysis was performed for all the stationary points to determine the character of minima or transition states. It was carefully checked that the vibrational mode associated with the imaginary frequency corresponds to the correct movement of involved atoms and, for most of the transition states, the correct nature of the intercepted transition state has been checked by using the IRC.[51–54] In line with previous reported works[55–58] were solvent effects were not included, free energy gas-phase calculations have been considered in this study. However, to support the reliability of those results and make easier the comparison with other works in literature,[21,22] the activation barrier relative to the rate-determining states of the most active catalyst **2 d** has been recalculated by taking into account the implicit solvation effects using the polarizable continuum model (PCM). The styrene oxide was mimic with cyclohexanone[22] and 2-Butanol, whose corresponding dielectric constants are both very similar to that determined for SO.[59] The calculated barriers are 24.7 and 25.1 kcal/mol for calculations done in cyclohexanone and 2-butanol, respectively. Even though solvent effects slightly reduce the energy barriers, those remain higher than that predicted for similar systems by Rostami[22] and Arayachukiat,[21] thus supporting the reliability of gas-phase free energies.

The ESM has been applied. This model associates the turnover frequency (TOF) to the energetic span of the cycle, δE, corresponding to the energy difference between the highest and lowest energy points along the potential energy surface of the overall catalytic cycle. Kozuch and Shaik[60,61] have been further extended the model by the inclusion of the ΔG_r of the reaction. δE_{ij} is therefore defined as:

According to this definition, if the *j-th* transition state lies after the *i-th* intermediate, then δE_{ij} is just the energy difference among them; if *j-th* transition state precedes the *i-th* intermediate, then δE_{ij} is their energy difference minus the ΔG_r. The highest δE_{ij} corresponds to the energy span of the cycle connecting the TOF-determining intermediate (TDI) and the TOF-determining transition state (TDTS).

Funding Sources

Project "e-Infrastructure CZ – LM2018140" funded by MEYS CR, and CzechNanoLab project LM2018110 funded by MEYS CR.

Supplementary Information

Supplementary Information to this article can be found online.

Acknowledgements

V. B. thanks IT4Innovations National Supercomputer Center, supported by The Ministry of Education, Youth and Sports from the Large Infrastructures for Research, Experimental Development and Innovations Project "e-Infrastructure CZ – LM2018140". CzechNanoLab project LM2018110 funded by MEYS CR is gratefully acknowledged for the financial support at CEITEC Nano Research Infrastructure. V. B. thanks the European Union – NextGenerationEU through the Italian Ministry of University and Research under PNRR – M4C2-I1.3 Project PE_00000019 "HEAL ITALIA".

Conflict of Interests

The authors declare no conflict of interest.

Data Availability Statement

The data that support the findings of this study are available in the supplementary material of this article.

Keywords: CO_2 conversion · cyclic carbonates · density functional theory · nicotinamidium iodides · organocatalysis

[1] J. Artz, T. E. Müller, K. Thenert, J. Kleinekorte, R. Meys, A. Sternberg, A. Bardow, W. Leitner, *Chem. Rev.* **2018**, *118*, 434–504.
[2] K. Jalama, *Catal. Rev. Sci. Eng.* **2017**, *59*, 95–164.
[3] W. H. Wang, Y. Himeda, J. T. Muckerman, G. F. Manbeck, E. Fujita, *Chem. Rev.* **2015**, *115*, 12936–12973.
[4] T. Sakakura, J. C. Choi, H. Yasuda, *Chem. Rev.* **2007**, *107*, 2365–2387.
[5] A. C. M. Loy, S. Y. Teng, B. S. How, X. Zhang, K. W. Cheah, V. Butera, W. D. Leong, B. L. F. Chin, C. L. Yiin, M. J. Taylor, G. Kyriakou, *Prog. Energy Combust. Sci.* **2023**, *96*, 101074.
[6] C. Huang, J. Wen, Y. Sun, M. Zhang, Y. Bao, Y. Zhang, L. Liang, M. Fu, J. Wu, D. Ye, L. Chen, *Chem. Eng. J.* **2019**, *374*, 221–230.
[7] J. Zhong, X. Yang, Z. Wu, B. Liang, Y. Huang, T. Zhang, *Chem. Soc. Rev.* **2020**, *49*, 1385–1413.
[8] S. Wesselbaum, V. Moha, M. Meuresch, S. Brosinski, K. M. Thenert, J. Kothe, T. Vom Stein, U. Englert, M. Hölscher, J. Klankermayer, W. Leitner, *Chem. Sci.* **2014**, *6*, 693–704.
[9] S. Wesselbaum, T. vom Stein, J. Klankermayer, W. Leitner, *Angew. Chem.* **2012**, *124*, 7617–7620.
[10] V. Butera, H. Detz, *Mater. Chem. Front.* **2021**, *5*, 8206–8217.
[11] H. Detz, V. Butera, *Mol. Catal.* **2023**, *535*, 112878.
[12] V. Butera, H. Detz, *Catal. Sci. Technol.* **2021**, *11*, 3556–3567.
[13] V. Butera, H. Detz, *ACS Appl Energ. Mater* **2022**, *5*, 4684–4690.
[14] S. Chen, W. H. Li, W. Jiang, J. Yang, J. Zhu, L. Wang, H. Ou, Z. Zhuang, M. Chen, X. Sun, D. Wang, Y. Li, *Angew. Chem. Int. Ed.* **2022**, *61*, e202114450.
[15] H. Rao, L. C. Schmidt, J. Bonin, M. Robert, *Nature* **2017**, *548(7665)*, 74–77.
[16] B. Alotaibi, S. Fan, D. Wang, J. Ye, Z. Mi, *ACS Catal.* **2015**, *5*, 5342–5348.
[17] I. Ritacco, M. Farnesi Camellone, L. Caporaso, H. Detz, V. Butera, *ChemCatChem* **2023**, *15*, e202201171.
[18] C. Liu, J. Kang, Z. Q. Huang, Y. H. Song, Y. S. Xiao, J. Song, J. X. He, C. R. Chang, H. Q. Ge, Y. Wang, Z. T. Liu, Z. W. Liu, *Nat. Commun.* **2021**, *12*, 1–10.
[19] V. D'Elia, A. W. Kleij, *Green Chem.* **2022**, *3*, 210–227.
[20] T. Yan, H. Liu, Z. X. Zeng, W. G. Pan, *J. CO_2 Util.* **2023**, *68*, 102355.
[21] S. Arayachukiat, C. Kongtes, A. Barthel, S. V. C. Vummaleti, A. Poater, S. Wannakao, L. Cavallo, V. D'Elia, *ACS Sustainable Chem. Eng.* **2017**, *5*, 6392–6397.
[22] A. Rostami, A. Ebrahimi, M. Al-Jassasi, S. Mirzaei, A. Al-Harrasi, *Green Chem.* **2022**, *24*, 9069–9083.
[23] A. Mitra, T. Biswas, S. Ghosh, G. Tudu, K. S. Paliwal, S. Ghosh, V. Mahalingam, *Sustain. Energy Fuels* **2022**, *6*, 420–429.
[24] S. Saengsaen, S. Del Gobbo, V. D'Elia, *Chem. Eng. Res. Des.* **2023**, *191*, 630–645.
[25] V. Butera, H. Detz, *ACS Omega* **2020**, *5*, 18064–18072.
[26] V. Butera, N. Russo, U. Cosentino, C. Greco, G. Moro, D. Pitea, E. Sicilia, *ChemCatChem* **2016**, *8*, 1167–1175.
[27] H. Detz, V. Butera, *J. Mol. Liq.* **2023**, *380*, 121737.
[28] S. Supasitmongkol, P. Styring, *Catal. Sci. Technol.* **2014**, *4*, 1622–1630.
[29] Y. Yang, Y. Guo, J. Yuan, H. Xie, C. Gao, T. Zhao, Q. Zheng, *ACS Sustainable Chem. Eng.* **2022**, *10*, 7990–8001.

[30] M. Asadi, K. Kim, C. Liu, A. V. Addepalli, P. Abbasi, P. Yasaei, P. Phillips, A. Behranginia, J. M. Cerrato, R. Haasch, P. Zapol, B. Kumar, R. F. Klie, J. Abiade, L. A. Curtiss, A. Salehi-Khojin, *Science (1979)* **2016**, *353*, 467–470.
[31] H. Tong, Y. Qu, Z. Li, J. He, X. Zou, Y. Zhou, T. Duan, B. Liu, J. Sun, K. Guo, *Chem. Eng. J.* **2022**, *444*, 135478.
[32] M. A. Emelyanov, A. A. Lisov, M. G. Medvedev, V. I. Maleev, V. A. Larionov, *Asian J. Org. Chem.* **2022**, *11*, e202100811.
[33] J. M. Ali, A. M. Mohammed, Y. S. Mekonnen, *J. Comput. Chem.* **2022**, *43*, 961–971.
[34] M. Razaghi, M. Khorasani, *J. CO_2 Util.* **2022**, *61*, 102028.
[35] S. Sopeña, E. Martin, E. C. Escudero-Adán, A. W. Kleij, *ACS Catal.* **2017**, *7*, 3532–3539.
[36] C. J. Whiteoak, A. Nova, F. Maseras, A. W. Kleij, *ChemSusChem* **2012**, *5*, 2032–2038.
[37] Y. Jiang, D. Li, Y. Zhao, J. Sun, *J. Colloid Interface Sci.* **2022**, *618*, 22–33.
[38] X. Yang, Z. Liu, P. Chen, F. Liu, T. Zhao, *J. CO_2 Util.* **2022**, *58*, 101936.
[39] H. Tong, Y. Qu, Z. Li, J. He, X. Zou, Y. Zhou, T. Duan, B. Liu, J. Sun, K. Guo, *Chem. Eng. J.* **2022**, *444*, 135478.
[40] J. Xu, A. Xian, Z. Li, J. Liu, Z. Zhang, R. Yan, L. Gao, B. Liu, L. Zhao, K. Guo, *J. Org. Chem.* **2021**, *86*, 3422–3432.
[41] R. Yan, K. Chen, Z. Li, Y. Qu, L. Gao, H. Tong, Y. Li, J. Li, Y. Hu, K. Guo, *ChemSusChem* **2021**, *14*, 738–744.
[42] K. Chen, R. Yan, Z. Li, W. Huang, L. Gao, T. Duan, H. Tong, Y. Li, J. Sun, K. Guo, *J. CO2 Util.* **2021**, *52*, 101663.
[43] L. Gao, Y. Zhou, Z. Li, J. He, Y. Qu, X. Zou, B. Liu, C. Ma, J. Sun, K. Guo, *J. CO2 Util.* **2022**, *65*, 102196.
[44] P. Jaramillo, L. R. Domingo, E. Chamorro, P. Pérez, *J. Mol. Struct.* **2008**, *865*, 68–72.
[45] M. J. Frisch, G. W. Trucks, H. B. Schlegel, G. E. Scuseria, M. A. Robb, J. R. Cheeseman, G. Scalmani., v. Barone, G. A. Petersson, H. Nakatsuji, X. Li, M. Caricato, A. V. Marenich, J. Bloino, B. G. Janesko, R. Gomperts, B. Mennucci, H. P. Hratchian, J. V. Ortiz, A. F. Izmaylov, J. L. Sonnenberg, D. Williams-Young, F. Ding, F. Lipparini, F. Egidi, J. Goings, B. Peng, A. Petrone, T. Henderson, D. Ranasinghe, v. G. Zakrzewski, J. Gao, N. Rega, G. Zheng, W. Liang, M. Hada, M. Ehara, K. Toyota, R. Fukuda, J. Hasegawa, M. Ishida, T. Nakajima, Y. Honda, O. Kitao, H. Nakai, T. Vreven, K. Throssell, J. A. Montgomery, J. E. P. Jr., F. Ogliaro, M. J. Bearpark, J. J. Heyd, K. E. N. Brothers, N. Kudin, v. N. Staroverov, T. A. Keith, R. Kobayashi, J. Normand, K. Raghavachari, A. P. Rendell, J. C. Burant, S. S. Iyengar, J. Tomasi, M. Cossi, J. M. Millam, M. Klene, C. Adamo, R. Cammi, J. W. Ochterski, R. L. Martin, K. Morokuma, O. Farkas, J. B. Foresman, D. J. Fox, "Citation | Gaussian.com," can be found under https://gaussian.com/citation/**2016**.
[46] J. P. Perdew, K. Burke, M. Ernzerhof, *Phys. Rev. Lett.* **1997**, *78*, 1396.
[47] J. P. Perdew, K. Burke, M. Ernzerhof, *Phys. Rev. Lett.* **1996**, *77*, 3865.
[48] M. Ernzerhof, G. E. Scuseria, *J. Chem. Phys.* **1999**, *110*, 5029.
[49] C. Adamo, V. Barone, *J. Chem. Phys.* **1999**, *110*, 6158.
[50] D. Andrae, U. Häußermann, M. Dolg, H. Stoll, H. Preuß, *Theor. Chim. Acta* **1990**, *77(2)*, 123–141.
[51] C. Gonzalez, H. Bernhard Schlegel, *J. Chem. Phys.* **1998**, *90*, 2154.
[52] K. Fukui, *J. Phys. Chem.* **1970**, *74*, 4161.
[53] V. Butera, N. Fukaya, J. C. Choi, K. Sato, Y. K. Choe, *Inorg. Chim. Acta* **2018**, *482*, 70–76.
[54] V. Butera, Y. Tanabe, Y. Shinke, T. Miyazawa, T. Fujitani, M. Kayanuma, Y.-K. Choe, *Int. J. Quantum Chem.* **2020**, *121*, e26494. 10.1002/qua.26494.
[55] W. Jiang, K. Zhu, H. Li, L. Zhu, M. Hua, J. Xiao, C. Wang, Z. Yang, G. Chen, W. Zhu, H. Li, S. Dai, *Chem. Eng. J.* **2020**, *394*, 124831.
[56] Q. Wang, X. Yao, Y. Geng, Q. Zhou, X. Lu, S. Zhang, *Green Chem.* **2015**, *17*, 2473–2479.
[57] A. M. da Costa Lopes, J. R. B. Gomes, J. A. P. Coutinho, A. J. D. Silvestre, *Green Chem.* **2020**, *22*, 2474–2487.
[58] Z. Zhu, H. Lin, M. Chi, X. Gao, Y. Feng, K. Yang, H. Lü, *Fuel* **2022**, *308*, 122070.
[59] M. A. Emelyanov, N. V. Stoletova, A. A. Lisov, M. G. Medvedev, A. F. Smol'Yakov, V. I. Maleev, V. A. Larionov, *Inorg. Chem. Front.* **2021**, *8*, 3871–3884.
[60] S. Kozuch, *Wiley Interdiscip. Rev.: Comput. Mol. Sci.* **2012**, *2*, 795–815.
[61] S. Kozuch, S. Shaik, *Acc. Chem. Res.* **2011**, *44*, 101–110.

Manuscript received: April 16, 2023
Revised manuscript received: May 28, 2023
Accepted manuscript online: June 21, 2023